Johnson et al., http://www.jcb.org/cgi/content/full/jcb.201406102/DC1

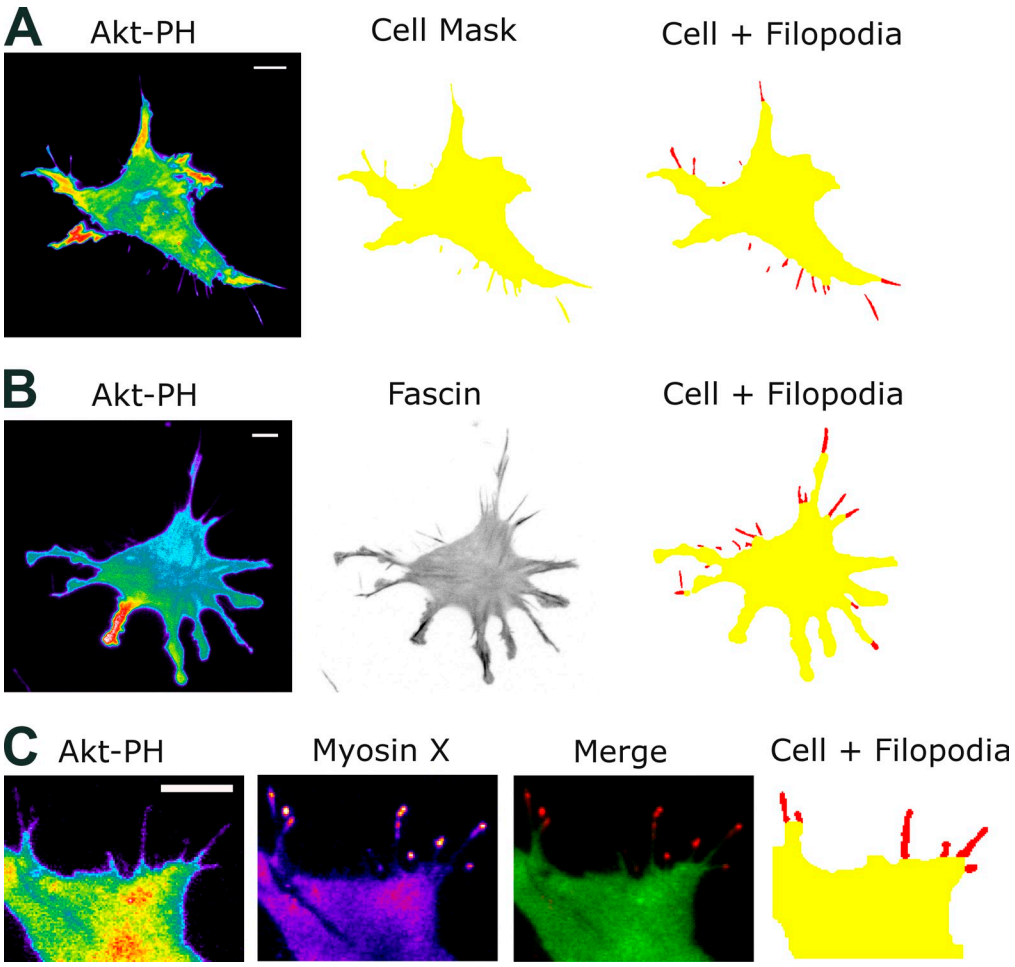

Figure S1. **Automated identification of filopodia.** (A) Putative filopodia are segmented (red; cell mask shown in yellow) by top-hat filtering of TIRF images. These structures may be tracked based on frame-to-frame overlap/proximity. (B) The structures thus identified tend to be enriched in FP-tagged fascin-1. (C) The putative filopodia are labeled by FP-tagged Myosin X at their tips. Bars, 10 µm.

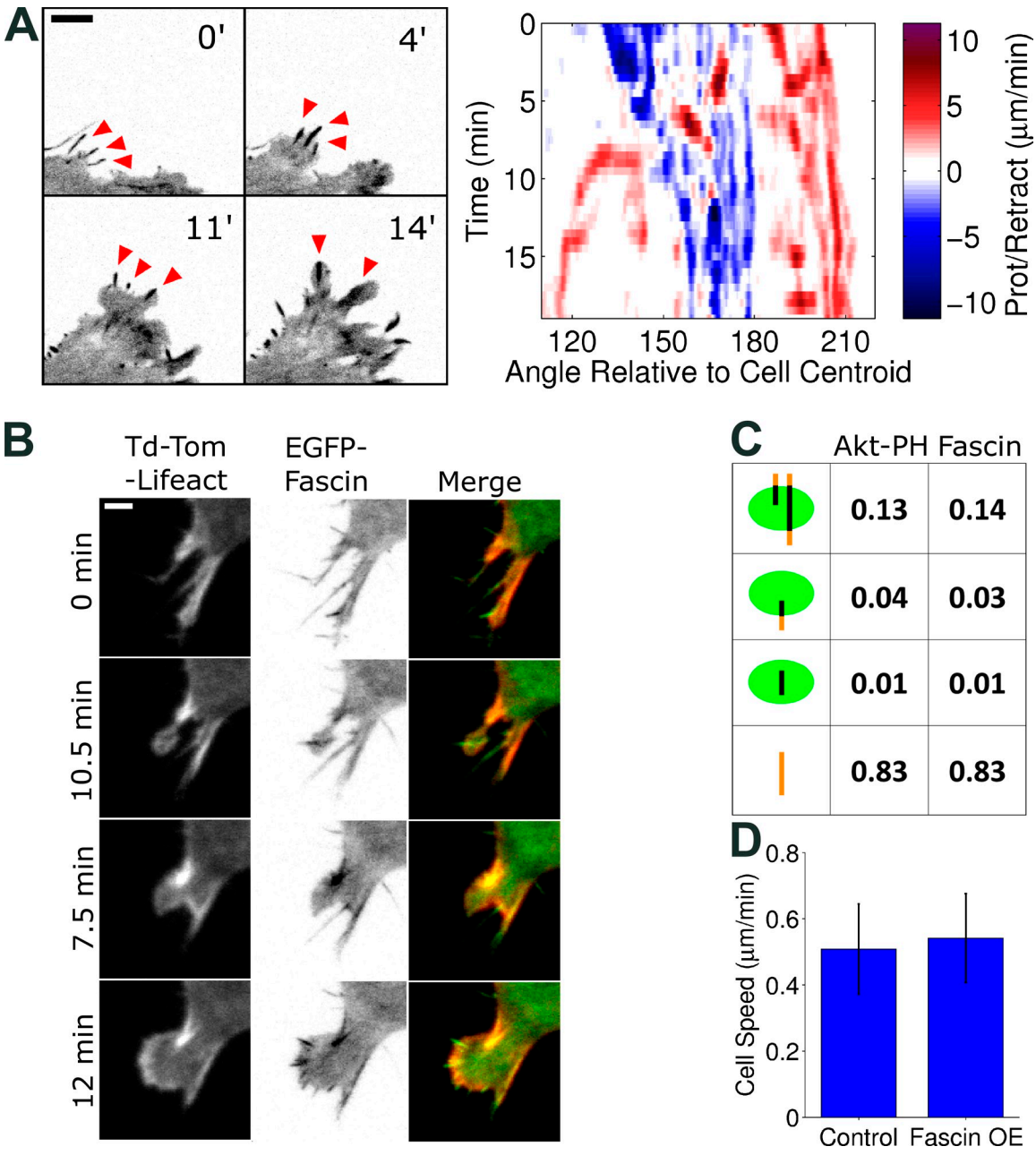

Figure S2. **F-actin bundles direct bifurcation of lamellipodia.** (A, left) Additional example from the cohort of cells analyzed in Fig. 2 A; TIRF montage of an NIH 3T3 fibroblast expressing EGFP-fascin (inverted grayscale), with prominent F-actin bundles marked by red arrows. Bar, 10 µm. (right) Corresponding spatiotemporal map of protrusion and retraction. The initiation of lamellipodial branching apparent in the latter two panels of the montage at left manifests on the map as an upside-down U shape (roughly, between 115° and 140° relative to the centroid starting at ~8 min in this time course). (B) TIRF montage of an NIH 3T3 coexpressing tdTomato (Td-Tom)-Lifeact and EGFP-fascin, illustrating F-actin organization in nascent lamellipodia and bundles. Bar, 5 µm. (C) Analysis of the percentages of filopodia that (from top to bottom): appear before an overlapping lamellipod; appear after, and persistent after, an overlapping lamellipod; appear after, and disappear during the lifetime of, an overlapping lamellipod; or appear and disappear with no overlap with lamellipodia. (D) Quantification of cell speed, by cell centroid tracking (sampled every 12 min) for control (n = 21) and fascin-overexpressing (OE; n = 31) cells. The data are presented as means ± 95% confidence interval.

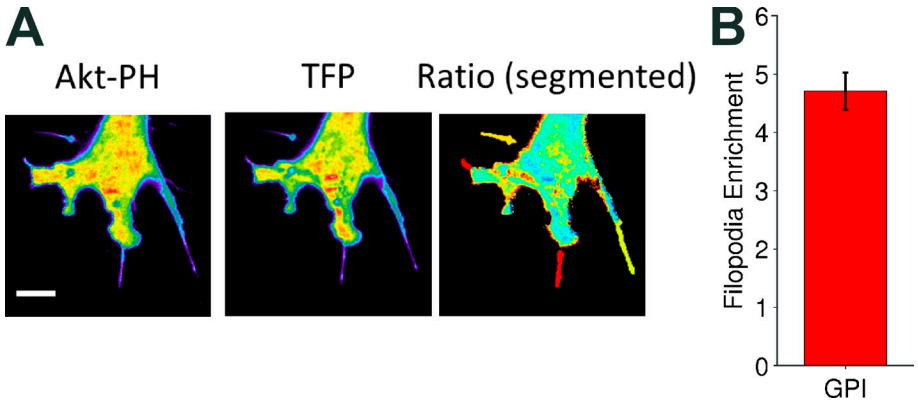

Figure S3. **Calculation of the enrichment ratio for filopodia.** (A) Putative filopodia were identified from volume marker (TFP) images as described under Materials and methods and Fig. S1. The mask associated with filopodia is dilated, and the mean intensity of each filopodial region is computed along with that of the cell interior. The ratio of those intensities (filopod/interior) is recorded. This procedure is then repeated for each region of pixels in the other channel, the mCherry-AktPH biosensor, for example. In this case, the enrichment ratio, *E* (the filopod/interior ratio of AktPH normalized by that of the volume marker) is used to assess the presence of PI3K signaling in the filopodia. Bar, 10 µm. (B) The value of *E* reflects both the extent of biosensor translocation (from the cytosol to the membrane) and the filopod geometry, effects that are not readily decoupled. Using a glycophosphatidylinositol (GPI)-anchored FP to uniformly label the outer leaflet of the plasma membrane, we estimated the relative enrichment of plasma membrane area relative to the volume of a filopodium. With FP-GPI in place of FP-AktPH, the mean value of *E* was 4.7 (n = 798 filopodia from nine cells; error bars indicate ±95% confidence interval), indicating a significant effect of geometry. Put another way, the ratio of AktPH/volume marker TIRF should not be used to compare relative 3′ phosphoinositide densities in filopodia versus elsewhere in the contact area.

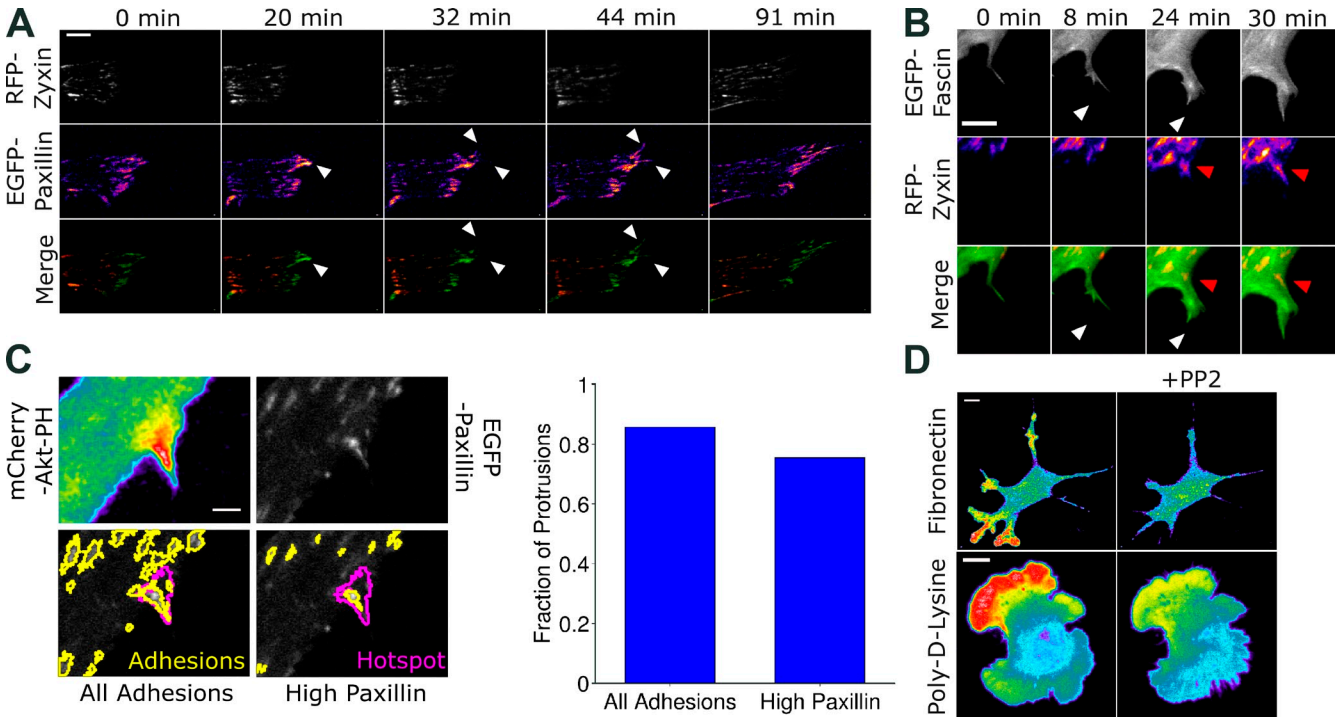

Figure S4. **TIRF imaging of adhesion dynamics.** (A) Two-color TIRF imaging of zyxin and paxillin in NIH 3T3 cells confirms that mature, zyxin-containing adhesions are found some distance behind the leading edge. Arrowheads indicate where adhesions form at the base of or beneath filopodia. (B) Two-color TIRF imaging of fascin and zyxin in NIH 3T3 cells confirms that zyxin-containing adhesions are typically located behind F-actin bundles at the periphery. White arrowsheads show filopod proceeding lamellipod formation, devoid of zxyin localization. Red arrowsheads show formation of zyxin-positive adhesions farther back in the cell. (C, left) Example of adhesion and PI3K signaling segmentation (*k*-means) for the protrusion shown in Fig. 4 B. Adhesions are outlined in yellow and the region of high PI3K signaling is outlined in magenta. All adhesions are regions that include pixels in the top two of 4 bins. High paxillin adhesions are defined as regions with pixels segmented in the highest bin only. (right) Fractions of protrusions over F-actin bundles with emergence of local PI3K signaling overlapping the two categories of adhesions (49 protrusion events in 13 cells, same cohort as in Fig. 4 B). (D) TIRF images of FP-AktPH–expressing NIH 3T3 cells, plated on either fibronectin or poly-lysine, before and after inhibition of Src-family kinases (PP2; 10 µM). The images are representative of 13 cells viewed for fibronectin and 19 cells viewed for poly-lysine. Bars: (A, B, and D) 10 µm; (C) 5 µm.

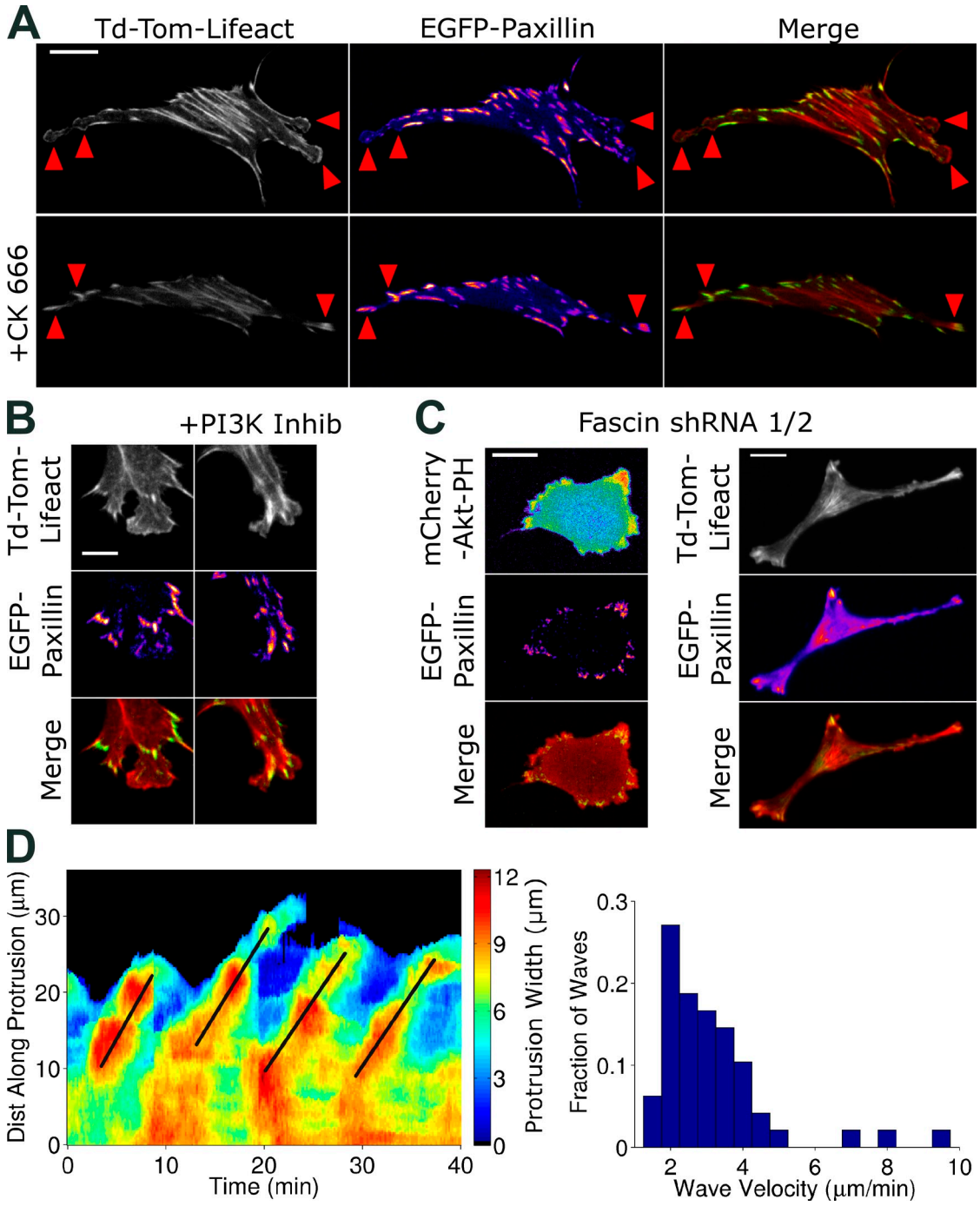

Figure S5. **Imaging interplay between protrusion and adhesion dynamics.** (A) Two-color TIRF imaging of Lifeact and paxillin before and after inhibition of Arp2/3 complex by 100 µM CK666. The arrows show where small adhesions were lost after collapse of lamellipodia. Td-Tom, td-Tomato. (B) Same as A but with inhibition (Inhib) of PI3K (1 µM PI3K-α inhibitor IV). (C) Two-color TIRF imaging of AktPH or Lifeact biosensor with tagged paxillin in cells depleted of fascin-1. (D, left) Kymograph of protrusion width during periodic protrusion waves as in Fig. 5 D. Lines are drawn through the waves and used to calculate the velocity of each wave. (right) Histogram indicating velocities of protrusion dilation waves (n = 48), estimated from kymograph as shown on the left. These were taken from high-resolution videos of 11 recurrent protrusions observed in six different cells. Bars: (A and C) 20 µm; (B) 10 µm.

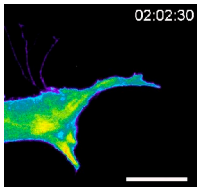

Video 1. **Time-lapse video of filopodia directing nascent lamellipodia, as depicted in Fig. 1 A.** TIRF microscopy images of an NIH 3T3 cell expressing EGFP-AktPH (pseudocolored) were acquired every 15 s for 132 min. Time stamp is shown in minutes, seconds, and milliseconds. Bar, 20 µm.

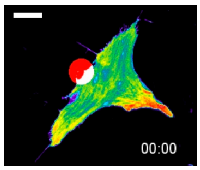

Video 2. **Time-lapse video of PI3K signaling and protrusion during photoactivation of Rac near filopodia, as depicted in Fig. 1 C.** TIRF microscopy images of an NIH 3T3 cell coexpressing mCerulean-PA-Rac and mCherry-AktPH (pseudocolored) were acquired every minute for 79 min. Time stamp shows hours and minutes. The red spots indicate the timing and area of photoactivation. Bar, 20 µm.

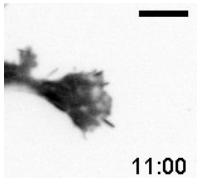

Video 3. **Time-lapse video of F-actin bundles directing lamellipodial protrusion, as depicted in Fig. 2 A.** TIRF microscopy images of an NIH 3T3 cell expressing EGFP-fascin (inverted grayscale) were acquired every 30 s for 21 min. Time stamp shows minutes and seconds. Bar, 10 µm.

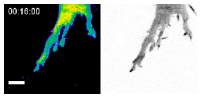

Video 4. **Time-lapse video of PI3K signaling and fascin localization during protrusion over an F-actin bundle, as depicted in Fig. 3 A.** TIRF microscopy images of an NIH 3T3 cell coexpressing mCherry-AktPH (left, pseudocolored) and EGFP-fascin (right, inverted grayscale) were acquired every 30 s for 67 min. Time stamp is shown in hours, minutes, and seconds. Bar, 10 µm.

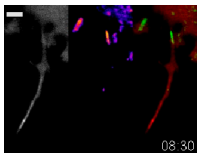

Video 5. **Time-lapse video of adhesion dynamics during protrusion over F-actin bundles, as depicted in Fig. 4 A.** TIRF microscopy images of an NIH 3T3 cell expressing mCherry-Fascin (left, grayscale) and EGFP-paxillin (center, pseudocolored) were acquired every 30 s for 20 min. Time is given in minutes and seconds. An overlay of the two channels is shown at right. Bar, 5 µm.

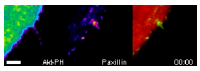

Video 6. **Time-lapse video showing adhesion formation and PI3K signaling during protrusion over actin bundles, as depicted in Fig. 4 B.** TIRF microscopy images of an NIH 3T3 cell expressing mCherry-AktPH (left) and EGFP-paxillin (right) were acquired every 30 s for 10 min. Time is given in minutes and seconds. An overlay of the two channels is shown at right. Bar, 5 µm.

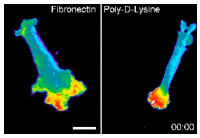

Video 7. **Time-lapse video showing ablation of localized PI3K signaling by FAK inhibition in cells plated on fibronectin but not on poly-lysine, as depicted in Fig. 4 C.** TIRF microscopy images of NIH 3T3 cells expressing FP-AktPH (pseudocolored), plated on either fibronectin (left) or poly-lysine (right), were acquired every 30 s for 17 min in separate experiments. At the indicated time, FAK activity was inhibited by addition of 10 µM FAK inhibitor II. Time is given in minutes and seconds. Bar, 20 µm.

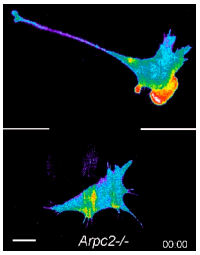

Video 8. **Time-lapse video showing ablation of localized PI3K signaling by Arp2/3 inhibition in uninduced cells, but not in cells with tamoxifen-induced knockout of Arpc2, as depicted in Fig. 5 C.** Fibroblasts with conditional knockout of the Arpc2 (p34) subunit of the Arp2/3 complex, transfected with FP-AktPH (pseudocolored), were either uninduced (top) or tamoxifen-induced (bottom). TIRF images were acquired every 30 s for 19 min in separate experiments. At the indicated time, the Arp2/3 complex was inhibited by addition of 100 µM CK666. Time is given in minutes and seconds. Bar, 20 µm.

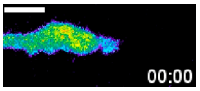

Video 9. **Time-lapse video of protrusion dilation waves, as depicted in Fig. 5 D.** TIRF microscopy images were of an NIH 3T3 cell expressing mCherry-AktPH (pseudocolored) were acquired every 10 s for 30 min. Time is given in minutes and seconds. Bar, 10 µm.

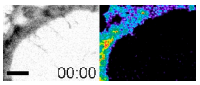

Video 10. **Time-lapse video of multiple F-actin bundles directing protrusions that coalesce to form a broad lamellipod, as depicted in Fig. 6 A.** TIRF microscopy images of an IA32 MEF coexpressing EGFP-fascin (inverted grayscale) and mCherry-AktPH (pseudocolored) were acquired every 30 s for 21 min. Time is given in minutes and seconds. Bar, 10 µm.